

Discharge Characteristics for Various Discharge Patterns under Negative Lightning Impulse Voltage in Vacuum

Fei Kong, Yusuke Nakano, Hiroki Kojima, Naoki Hayakawa

Department of Electrical Engineering and Computer Science, Nagoya University
Furo-cho, Chikusa-ku, Nagoya, 464-8603, Japan

Toshinori Kimura and Mitsuru Tsukima

Mitsubishi Electric Corporation
Advanced Technology R&D Center
8-1-1, Tsukaguchi-honmachi, Amagasaki, 661-8661, Japan

ABSTRACT

In order to develop higher voltage vacuum interrupters (VIs), electrical insulation performances in vacuum should be improved. The discharge in VI has various and complex patterns, such as breakdown in vacuum gap and surface flashover on a solid insulator. In this paper, we investigated three discharge patterns: the discharge in vacuum gap, the discharge in vacuum gap via shield, and the surface flashover on solid insulator, respectively. By measuring shield potential and insulator surface potential, we analyzed the discharge characteristics for various patterns, and clarified the relevant discharge development process. We found that the breakdown development process in vacuum gap depends on the gap length and the surface flashover development process on a solid insulator depends on the applied voltage and surface distance.

Index Terms — Vacuum, breakdown, floating electrode, surface flashover, alumina ceramics

1 INTRODUCTION

WITH the development of vacuum insulation technology, vacuum circuit breakers (VCBs) / vacuum interrupters (VIs) have been utilized worldwide up to the 84 kV class in medium voltage systems and distribution power networks. For higher voltage class VIs, electrical insulation performances in vacuum should be improved [1]. When the internal insulation fails in VI, the discharge has various and complex patterns, such as the breakdown in vacuum gap between main contacts, or between contacts and shield, and the surface flashover on a solid insulator [2, 3]. Reference [3] shows the voltage shape characteristics of various discharge patterns in VI, however, the relationship between discharge waveforms (voltage, current, shield potential) and breakdown or surface flashover development process in vacuum has not been clarified enough.

In the present paper, we proposed several simple electrode configurations to investigate the discharge patterns which can occur in VI as shown in Figure 1. The cathode-anode (c-a) pattern represents the breakdown in vacuum gap between main contacts, the cathode-shield-anode (c-s-a) pattern represents the breakdown in vacuum

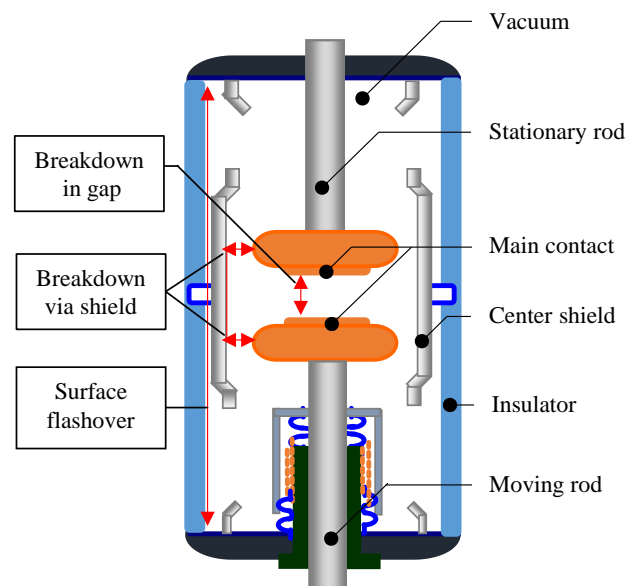


Figure 1. Discharge patterns in VI.

gap via center shield (floating electrodes), and the cathode-insulator-anode (c-i-a) pattern represents the surface flashover on a solid insulator. Here, we focused on the discharge development process for different discharge patterns in order to understand the fundamental discharge mechanisms in vacuum. We measured the electrical parameters (e.g. applied voltage, anode current, shield potential, surface potential on insulator, etc.), and the discharge characteristics and mechanisms for various discharge patterns in vacuum were investigated.

2 EXPERIMENTAL SETUP

2.1 TEST CIRCUIT

Figure 2 shows the experimental circuit with measurement systems. The vacuum pressure in the chamber is set at 10^{-5} Pa order. The impulse generator provides a standard negative lightning impulse voltage ($-1.2/50 \mu\text{s}$). We applied the negative impulse voltage between electrodes to be described in section 2.2. We measured the applied voltage waveform with a voltage divider, the anode current with a high frequency current transformer (CT). We also measured the shield potential and surface potential on a solid insulator by high voltage probe in the cases of c-s-a and c-i-a, respectively. In addition, the still image of discharge is observed with a digital camera and the light intensity with a photomultiplier tube (PMT).

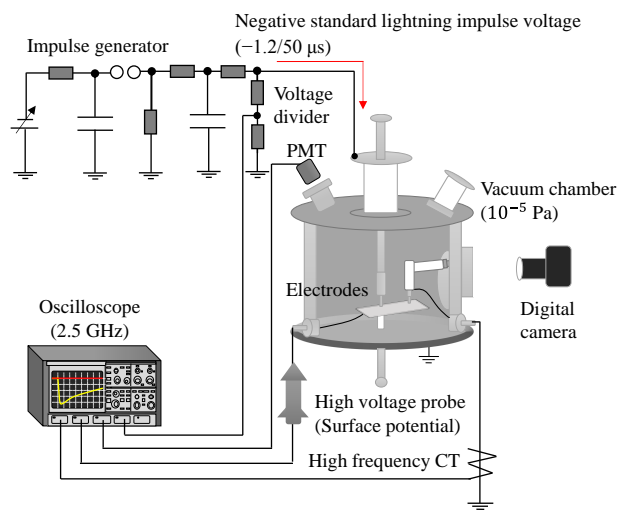


Figure 2. Experimental setup with measurement systems.

2.2 ELECTRODE CONFIGURATIONS

Based on the possible discharge patterns in Figure 1, three electrode configurations are assembled as shown in Figure 3. For each configuration, the cathode and the anode are rod shape with of a diameter of 2 mm, whose material is stainless steel. The shapes of shield and insulator are rectangular plate. We applied the negative impulse voltage to the cathode, and the anode is grounded.

Figure 3a shows the electrode configuration of c-a. The gap length g is set from 0.25 to 0.75 mm. In addition, we put a floating electrode as a shield below the vacuum gap,

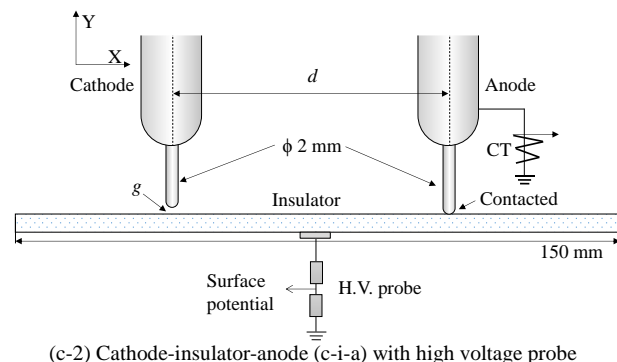
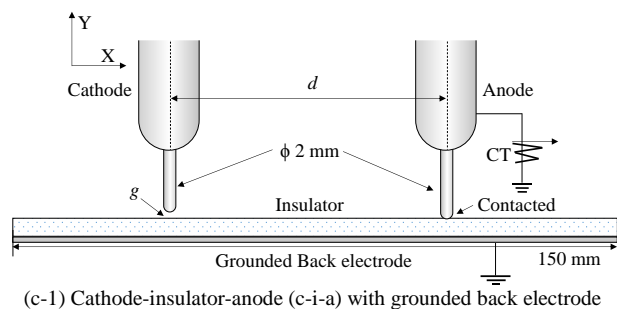
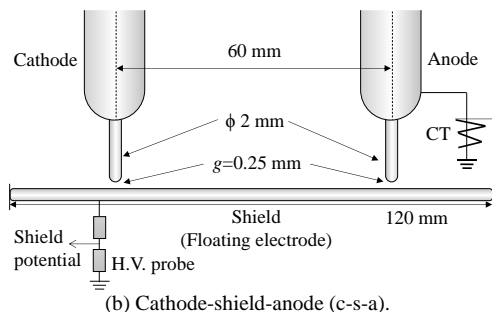
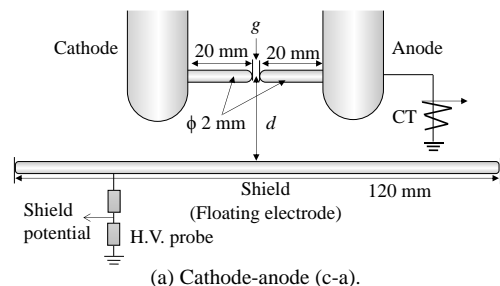


Figure 3. Electrode configurations for various discharges.

and the distance d between the vacuum gap and the shield is set from 18.5 to 38.5 mm. The shield is made of stainless steel, whose dimension is $120 \text{ mm} \times 60 \text{ mm} \times 2 \text{ mm}^t$. The shield potential is measured by a high voltage probe (input impedance: $100 \text{ M}\Omega$).

Figure 3b shows the electrode configuration of c-s-a. The shield is placed below the rod electrodes with a gap of 0.25 mm. The shield potential is also measured by the high voltage probe.

Figure 3c-1 shows the electrode configuration of c-i-a. The insulator is alumina ceramics (Al_2O_3 , purity: 92%), whose dimension is $150 \text{ mm} \times 150 \text{ mm} \times 5 \text{ mm}^t$. The gap length g between the cathode and the insulator is 0 to 0.5 mm, and the anode and the insulator are contacted. The surface distance d between the cathode and the anode is set from 20 to 60 mm. A grounded back electrode is set behind the insulator. In addition, in order to investigate the flashover development process, we set a high voltage probe behind the insulator as shown in Figure 3c-2. The high voltage probe is set in the midpoint between the cathode and the anode, which enables us to measure the surface potential of insulator. The high voltage probe can be considered as a floating electrode, because it has a high input impedance of $100 \text{ M}\Omega$.

3 EXPERIMENTAL RESULTS AND DISCUSSION

3.1 BREAKDOWN IN VACUUM GAP

Figure 4 shows the still image of breakdown between cathode and anode (c-a). Figure 5 shows the discharge waveforms in the case of c-a breakdown. Once the breakdown initiates, the applied voltage decreases rapidly, and simultaneously the anode current increases up to about 150 A. We define the time from breakdown initiation to the first peak of anode current as the breakdown development time T_{BD} . In this period, the discharge is initiated by the plasma produced at the cathode surface [4]. Figure 6 shows the breakdown development time T_{BD} for various gap lengths. We can find that T_{BD} became long proportionally with the increase in the gap length. The breakdown development time depends on the cathode plasma expansion velocity. In Figure 6, the slope represents that the cathode plasma velocity is $3.1 \times 10^4 \text{ m/s}$, which agrees with the

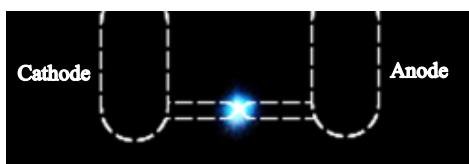


Figure 4. Still image of breakdown for c-a ($V_{BD} = -20.8 \text{ kV}$, $g=0.25 \text{ mm}$, $d=28.5 \text{ mm}$)

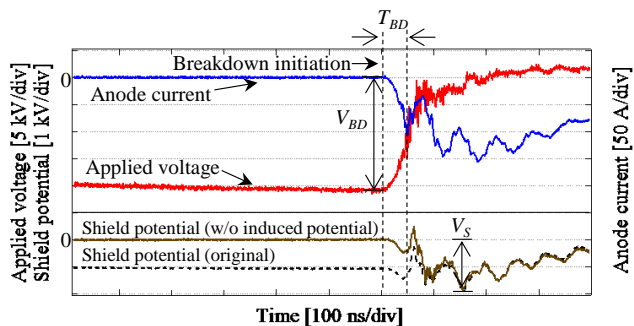


Figure 5. Discharge waveforms of breakdown for c-a ($V_{BD} = -20.8 \text{ kV}$, $g=0.25 \text{ mm}$, $d=28.5 \text{ mm}$).

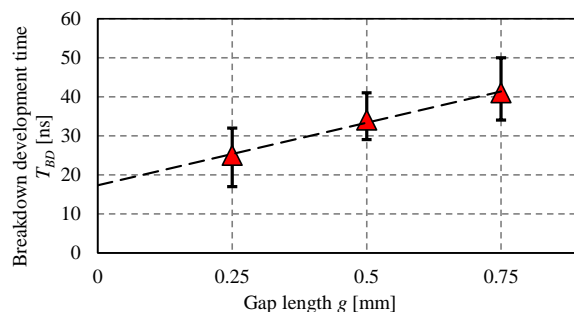


Figure 6. Breakdown development time T_{BD} for various gap in c-a breakdown.

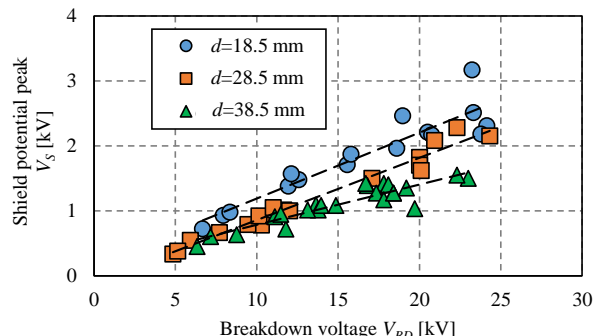


Figure 7. Relation between V_S and V_{BD} for c-a breakdown.

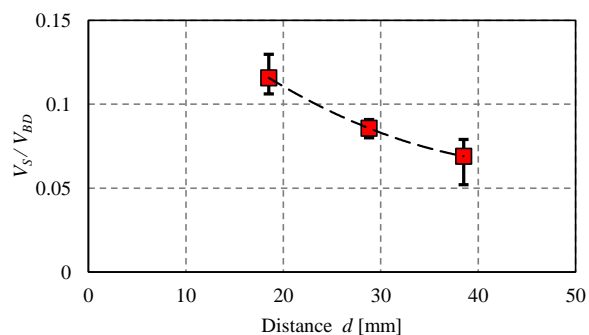


Figure 8. Relation between V_S / V_{BD} and d for c-a breakdown.

cathode plasma expansion velocity of $1\text{-}3 \times 10^4 \text{ m/s}$ in the process that the cathode plasma reached the anode [5, 6].

The transition of shield potential is also shown in Figure 5, where the induced potential by the applied voltage due to the capacitance between shield and ground before breakdown is deducted. Once the breakdown occurs, the negative shield potential appears because the electron flow produced by the discharge reaches the shield [7]. In Figure 7, the shield potential peak V_S increases proportionally with the increase in breakdown voltage V_{BD} , which indicates that the electron quantity produced by the discharge depends on V_{BD} . In Figure 8, we focus on the relation between V_S / V_{BD} and the distance d . We can find V_S / V_{BD} decreases with increasing d . It is because that, if electrons spread isotropically from the gap toward the surrounding vacuum space [8], the number of electrons reaching the shield depends on the solid angle of the shield seen from the vacuum gap. Less electrons reached the shield for the larger d with a smaller solid angle.

3.2 BREAKDOWN VIA FLOATING ELECTRODE

For the c-s-a pattern, Figure 9 shows a still image of discharge and temporal development of shield potential for partial breakdown (PB) between cathode-shield (c-s). In Figure 9a, a weak light emission is observed at the gap between the cathode and the shield only, which infers that PB occurs between the cathode and the shield. As shown in Figure 9b, the shield potential increases rapidly up to the

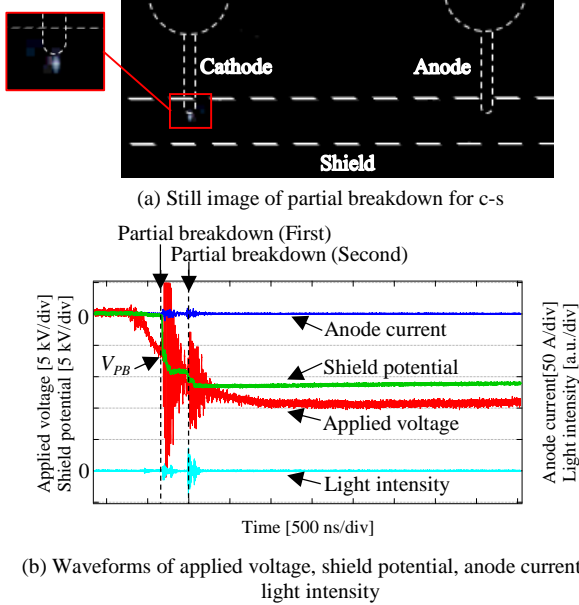


Figure 9. Still image and transition of shield potential for partial breakdown via cathode-shield (c-s) ($V_{PB} = -6.5$ kV).

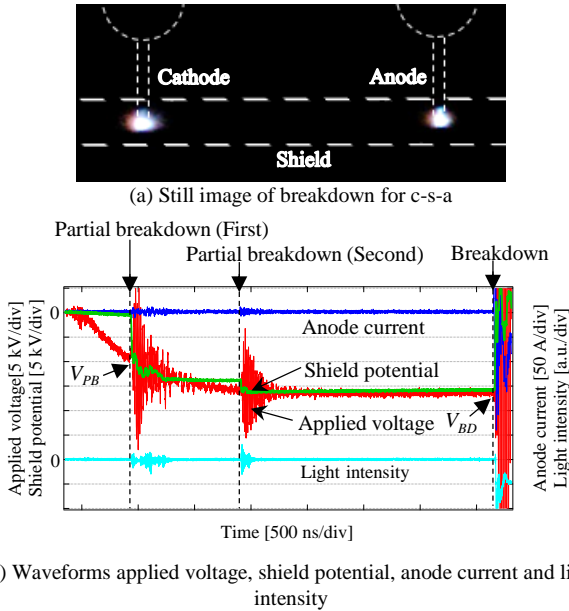


Figure 10. Still image and transition of shield potential for breakdown via cathode-shield-anode (c-s-a) ($V_{PB} = -9.4$ kV, $V_{BD} = -16.4$ kV).

instantaneous applied voltage once PB occurs. Afterwards, in spite of quenching the discharge between c-s, the shield potential remains to a constant value, since the shield is a floating electrode. The second PB occurs at 320 ns after the first PB, which results in the enhancement of the shield potential. The anode current is not measured, because the discharge channel is not formed between the shield and the anode even after twice PB.

Figure 10 shows the still image of discharge and temporal development of shield potential for breakdown (BD) via cathode-shield-anode (c-s-a). In Figure 10a, strong light emissions are observed both at the gaps of cathode-shield and shield-anode, which represents the breakdown occurred completely. Figure 10b represents that twice PB between cathode and shield occurred before BD. Then, the discharge channel was formed between shield and anode as well as between cathode and shield, and the anode current increased up to more than 100 A. Therefore, the shield potential development enabled us to clarify two kinds of discharge patterns (c-s, c-s-a) and to recognize that BD via c-s-a occurs subsequently to PB (c-s).

3.3 SURFACE FLASHOVER ON INSULATOR

For the c-i-a pattern, Figure 11 shows the still image of surface flashover and waveforms of applied voltage, anode current, light intensity for the electrode configuration in Figure 3c-1. In Figure 11a, the light emission is observed on the insulator surface between the cathode and the anode, which represents the surface flashover occurred. In Figure 11b, surface flashover started with the explosive electron emission (EEE) at the cathode and the applied voltage began to fall down [9]. During the surface flashover development, the anode current increased to more than 100A and the applied voltage fell to almost zero, which suggests that a conductive channel between cathode and anode was formed.

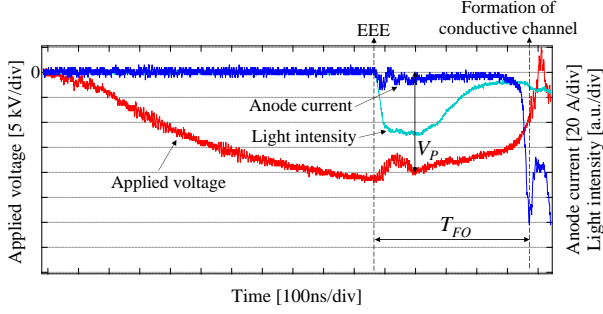
Figure 12 shows the transition of surface potential on the insulator with the high voltage probe in Figure 3c-2 when surface flashover occurred. Before EEE, an induced surface potential is measured due to the capacitance of insulator. Once EEE occurs, because the secondary electron emission efficiency of the insulator is less than 1, the surface potential is negative and increases gradually to about -3 kV. Afterwards, the surface potential decreases with the formation of conductive channel on the insulator surface.

Therefore, we define the time from EEE to the formation of conductive channel as the surface flashover development time T_{FO} . In addition, we define the voltage peak after EEE as V_p . Figure 13 shows the relation between T_{FO} and V_p for various surface distance in Figure 3c-1. T_{FO} decreased with increasing V_p for all $d = 20$ -60 mm. Furthermore, we can find that T_{FO} is proportional to V_p^{-2} , which is consistent with the experimental data of the parallel plane electrodes configuration [10].

After the EEE initiation, with electron-stimulated outgassing from insulator, the plasma density above the insulator surface increases with gaseous ionization, and

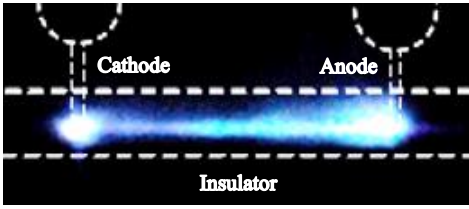


(a) Still image of surface flashover for c-i-a

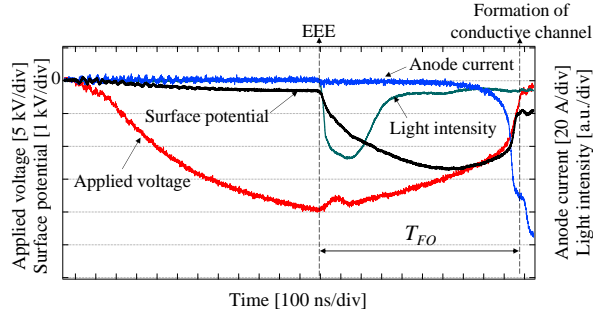


(b) Waveforms of applied voltage, anode current and light intensity

Figure 11. Still image and discharge waveforms for surface flashover via cathode-insulator-cathode (c-i-a) with grounded back electrode ($V_p = -19.4$ kV, $g=0.5$ mm, $d=60$ mm).



(a) Still image of surface flashover for c-i-a



(b) Waveforms of applied voltage, surface potential, anode current and light intensity

Figure 12. Still image and discharge waveforms for surface flashover via cathode-insulator-cathode (c-i-a) with high voltage probe ($V_p = -18.8$ kV, $g=0.5$ mm, $d=60$ mm).

eventually leads to the formation of conductive channel [10-12]. The electron-stimulated outgassing can be promoted with the higher voltage, which makes the shorter T_{FO} . According to the electron-stimulated outgassing model in the parallel plane electrode configuration, the electron-stimulated outgassing depends on the electric field E_y on the insulator surface perpendicular to the insulator which is produced by charge on the insulator surface, and T_{FO} is reported to be proportional to E_y^{-2} from the theoretical calculation [10]. On the other hand, in our rod-plane electrode configuration in Figure 3c-1, we confirmed that

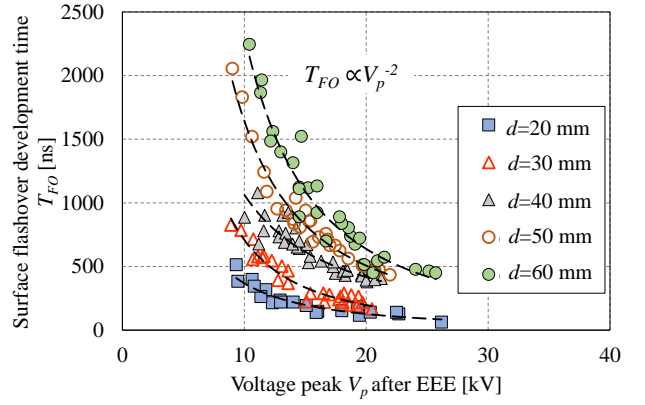


Figure 13. Relation between surface flashover development time T_{FO} and voltage peak V_p after EEE for electrode configuration in Figure 3c-1.

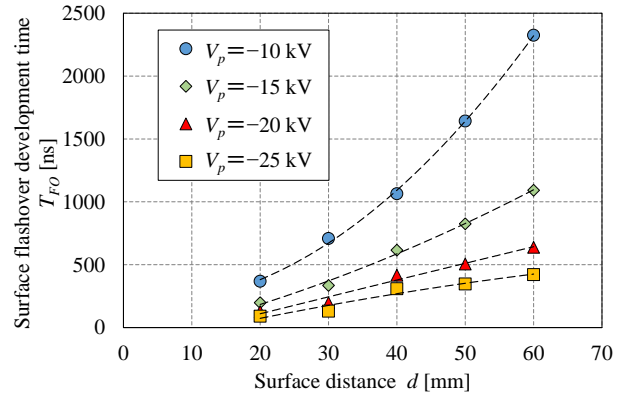


Figure 14. Relation between surface flashover development time T_{FO} and surface distance d for electrode configuration in Figure 3c-1.

the electric field strength on the insulator surface by applied voltage is higher than that by the measured surface charging potential, and its direction is almost perpendicular to the insulator surface. Thus, E_y is mainly decided by the applied voltage, i.e. V_p . Hence, T_{FO} is proportional to V_p^{-2} in the rod-plane electrode configuration.

Figure 14 shows the relation between T_{FO} and surface distance d for various V_p . T_{FO} increased with increasing surface distance d for a certain V_p . Based on the relation between T_{FO} and d , the surface distance can be estimated from the measurement of T_{FO} and V_p .

4 SUMMARY

In this paper, according to the possible discharge phenomena in VI, we discussed discharge characteristics for various discharge patterns using several simple electrodes configurations. The main results are summarized as follows:

(1) For the breakdown in pure vacuum gap (c-a), the breakdown development time T_{BD} became longer when the gap length increased. In addition, we found that the shield potential near the vacuum gap increased once breakdown occurred, because electron flow produced by discharge spread to the shield. Furthermore, less electrons reached the

shield with the increase in the distance between vacuum gap and shield, because the electrons can spread isotropically from the gap toward vacuum space.

(2) The breakdown in vacuum gap via shield (c-s-a) has two cases: partial breakdown (PB) and breakdown (BD). Firstly, PB occurred between cathode and shield (c-s) only. If the applied voltage is sufficiently high, the breakdown between shield and anode (c-s-a) occurred. In the PB, the shield potential increased up to the applied voltage rapidly.

(3) For the surface flashover on a solid insulator with rod-plane electrodes (c-i-a), the surface flashover development time T_{FO} is considered as conductive channel formation time. The conductive channel formation time becomes short with the increase in the perpendicular component of the electric field on the insulator surface by the applied voltage, because the higher electric field can promote electron-stimulated outgassing from the insulator surface. The surface flashover development time T_{FO} increased with increasing surface distance d . We can estimate the surface distance based on the relation between T_{FO} , V_p and d .

REFERENCES

- [1] H. Okubo, "Development of Electrical Insulation Techniques in Vacuum for Higher Voltage Vacuum Interrupters", the 22nd International Symposium on Discharges and Electrical Insulation in Vacuum, pp. 7-12, 2006.
- [2] Irina N. Poluyanovo, Vladimir A. Bugayov and Anton V. Vykhotdsev, "Voltage Shape of Impulse Breakdown in Internal Insulation of VI", the 26th International Symposium on Discharges and Electrical Insulation in Vacuum, pp.441-444, 2014.
- [3] V. A. Nevrovsky and L. A. Rylskaya, "Limiting Electric Strength of Vacuum Electrode Systems Including Combined Breakdown", the 20th International Symposium on Discharges and Electrical Insulation in Vacuum, pp.190-193, 2002.
- [4] I. D. Chalmers and B. D. Phukan, "Photographic Observations of Impulse Breakdown in Short Vacuum Gaps", J. Phys. D: Appl. Phys., Vol.12, pp.1285-1292, 1979.
- [5] Gennady A. Mesyats and D. I. Proskurovsky, "Pulsed Electrical Discharge in Vacuum", 1st ed., Springer-Verlag, pp.118-120, 1989.
- [6] M. B. Bochkarev, Yu. A. Zemskov and I. V. Uimanov, "High Speed and Spectroscopic Investigation of 300kV Pulsed Vacuum Spark in Centimeter Gap", the 24th International Symposium on Discharges and Electrical Insulation in Vacuum, pp.72-75, 2010.
- [7] I. L. Muzyukin, "On Plasma Flow Parameters of Nanosecond Vacuum Spark Discharge", the 24th International Symposium on Discharges and Electrical Insulation in Vacuum, pp.517-519, 2010.
- [8] E. Hantzsche, "Theory of The Expanding Plasma of Vacuum Arcs", J. Phys. D, Appl. Phys. Vol.24, pp.1339-1353, 1991.
- [9] Y. Nakano, H. Kojima, K. Tsuchiya and N. Hayakawa, "Transient Charging for Impulse Surface Flashover Development in Vacuum", the 26th International Symposium on Discharges and Electrical Insulation in Vacuum, pp.57-60, 2014.
- [10] R. A. Anderson and J. P. Brainard, "Mechanism of Pulsed Surface Flashover Involving Electron-stimulated Desorption", Journal of Applied Physics, Vol.51, No.3, pp.1414-1421, 1980.
- [11] A. Sivathanu Pillai and Reuben Hackam, "Surface Flashover of Solid Dielectric in Vacuum", Journal of Applied Physics, Vol.53, No.4, pp.2983-2987, 1982.
- [12] Andreas A. Neuber, M. Butcher, H. Krompholz, Lynn L. Hatfield and Magne Kristiansen, "The Role of Outgassing in Surface Flashover under Vacuum", IEEE Transactions on Plasma Science, Vol.28, No.5, pp.1593-1598, 2000.



Fei Kong (S'14) was born on 13 July in 1987. He received the M.S. degree in electrical engineering from Beijing Jiaotong University, Beijing, China, in 2011. Currently, he is a Ph.D. candidate of Nagoya University (MEXT scholarship) at the Department of Electrical Engineering and Computer Science. His major research interests include discharges phenomenon and electrical insulation in vacuum. He is a member of IEE of Japan.



Yusuke Nakano (S'12) was born on 5 March in 1988. He received the Ph.D. degree in electrical engineering from Nagoya University. He received ICEPE-ST Wang Jimei Best Paper Award in 2013. His major research interests include surface flashover and electrical insulation in vacuum. Dr. Nakano is a member of IEE of Japan.



Hiroki Kojima (M'11) was born on 7 December 1975. He received the Ph.D. degree in 2004 in energy engineering and science from Nagoya University. Since 2004, he has been at Nagoya University and presently he is an Associate Professor of Nagoya University at the Department of Electrical Engineering and Computer Science. Dr. Kojima is a member of IEE of Japan.



Japan.

Naoki Hayakawa (M'90) was born on 9 September 1962. He received the Ph.D. degree in 1991 in electrical engineering from Nagoya University. Since 1990, he has been at Nagoya University and presently he is a Professor of Nagoya University at the Department of Electrical Engineering and Computer Science. From 2001 to 2002, he was a guest scientist at the Forschungszentrum Karlsruhe/Germany. Prof. Hayakawa is a member of CIGRE and IEE of



Toshinori Kimura was born in Japan on June 27, 1964. He received the B.S. and M.S. degrees in physics from Hokkaido University in 1988 and 1990, respectively. In 1990, he joined Mitsubishi Electric Corporation. Presently, he is engaged in researching arc physics and the development of vacuum circuit breakers in Advanced Technology R&D Center. Mr. Kimura is a member of IEE of Japan.



Mitsuru Tsukima was born in Kyoto, Japan, on June 2, 1970. He received the B.S. and M.S. degrees in applied physics from Osaka University, Osaka, Japan, in 1994 and 1996, respectively. He joined the Advanced Technology R&D Center, Mitsubishi Electric Corporation, Amagasaki, Japan, in 1996. He is currently working on circuit breakers and related technologies. Dr. Tsukima is a member of IEE of Japan.